2-2006

Trap Loss in a Dual-Species Rb-Ar* Magneto-Optical Trap

H. C. Busch
Old Dominion University

M. K. Shaffer
Old Dominion University

E. M. Ahmed
Old Dominion University

C. I. Sukenik
Old Dominion University, csukenik@odu.edu

Original Publication Citation

Busch, H.C., Shaffer, M.K., Ahmed, E.M., & Sukenik, C.I. (2006). Trap loss in a dual-species Rb-Ar* magneto-optical trap. *Physical Review A, 73*(2), 23406. doi: 10.1103/PhysRevA.73.023406

Trap loss in a dual-species Rb-Ar* magneto-optical trap

H. C. Busch, M. K. Shaffer, E. M. Ahmed, and C. I. Sukenik
Department of Physics, Old Dominion University, Norfolk, Virginia 23529, USA
(Received 5 October 2005; revised manuscript received 29 December 2005; published 9 February 2006; publisher error corrected 21 February 2006)

We have investigated trap loss in a dual-species magneto-optical trap (MOT) comprised of ^{85}Rb and metastable ^{40}Ar. We measure the trap loss rate coefficients for each species due to the presence of the other as a function of trap light intensity. We clearly identify both Penning ionization of Rb by Ar^* and associative ionization to form the molecular ion $RbAr^+$ as two of the trap loss channels. We have also measured the trap loss rate coefficient for the Ar^* MOT alone and observe production of Ar^+ and Ar_2^+ ions.

DOI: 10.1103/PhysRevA.73.023406 PACS number(s): 32.80.Pj, 32.80.Lg, 33.80.Ps

I. INTRODUCTION

In recent years, interest in the interaction between dissimilar atoms at ultracold temperatures has been increasing. Motivation for such studies includes the production of polar molecules for quantum computation [1], sympathetic cooling of one species by another [2], heteronuclear photoassociative spectroscopy [3], multispecies quantum-degenerate systems [4], and cold chemistry [5]. Whereas the first excited state of homonuclear dimers with internuclear separation R is characterized by a long-range $1/R^3$ resonant dipole interaction, for the heteronuclear case it is the much-shorter-range $1/R^6$ van der Waals interaction which typically dominates, resulting in a different set of collision dynamics. Furthermore, if one of the atoms is in a highly energetic excited state, as is the case for metastable noble-gas atoms in a trap, then heteronuclear ionization may occur, resulting in an additional channel for trap loss beyond the familiar inelastic collision mechanisms which can eject atoms from a trap.

In a previous paper [6], we reported on the first dual-species magneto-optical trap (MOT) to simultaneously confine alkali-metal atoms (^{85}Rb) and metastable noble-gas atoms ($^{40}Ar^*$). Here we report measurements of the total trap loss rate coefficients for each species due to the presence of the other and identify heteronuclear Penning and associative ionization as two of the trap loss mechanisms. We also present results of trap loss measurements in the Ar^* MOT alone.

II. DETERMINING TRAP LOSS

Loss of atoms in a magneto-optical trap arises both from collisions between cold, trapped atoms and from collisions between trapped atoms and background gas in the vacuum chamber [7]. These losses can be quantified by observing the transient loading or decay of atoms in the trap. Details of this analysis have been discussed by several groups recently [8,9] and are briefly reviewed here.

The time evolution for the number of Rb atoms in a dual-species MOT comprised of both Rb and Ar^* is governed by the differential equation

$$\frac{dN_{\mathrm{Rb}}}{dt} = L - \gamma N_{\mathrm{Rb}} - \beta_{\mathrm{Rb}} \int_V n_{\mathrm{Rb}}^2 d^3r - \beta'_{\mathrm{Rb\text{-}Ar^*}} \int_V n_{\mathrm{Rb}} n_{\mathrm{Ar^*}} d^3r, \tag{1}$$

where L is the Rb MOT loading rate, γ is the loss rate coefficient arising from collisions with hot background atoms (mainly ground-state argon in this case), β_{Rb} is the loss rate coefficient arising from collisions between two ultracold rubidium atoms in the trap, and finally, $\beta'_{\mathrm{Rb\text{-}Ar^*}}$ is the loss rate coefficient arising from collisions between ultracold Rb atoms and trapped, ultracold Ar^* atoms. The integral is taken over the volume V. The time evolution for Ar^* in the trap obeys an analogous equation. Note, however, that there is no *a priori* reason that the interspecies trap loss coefficient $\beta'_{\mathrm{Ar^*\text{-}Rb}}$, describing the loss of Ar^* due to the presence of Rb, should be the same as $\beta'_{\mathrm{Rb\text{-}Ar^*}}$. The single-species rate β_{Rb} has been measured by several groups [10,11]; although Ar^* MOTs have been investigated [12], only order-of-magnitude estimates of $\beta_{\mathrm{Ar^*}}$ have been published [13]. It is $\beta'_{\mathrm{Rb\text{-}Ar^*}}$ and $\beta'_{\mathrm{Ar^*\text{-}Rb}}$ that we are primarily interested in here.

We find in our MOT that the spatial distribution for both the Rb and Ar^* MOT is well described by a Gaussian distribution. Neither MOT reaches the density-limited regime at any point during loading in the experiments reported here. We define the density $n(r,t)$ by writing

$$n(r,t) = n_0(t) e^{-2[r/\omega(t)]^2}. \tag{2}$$

Strictly speaking, ω is a function of time; however, below the density-limiting regime, for which $n < n_c$, where n_c is the "critical" density, the MOT tends to fill by adding atoms at constant volume (the "constant-volume regime") and so we let $\omega(t) = \omega$.

In order to determine the interspecies trap loss, we must first characterize the single-species interactions. By setting $\beta' = 0$, substituting Eq. (2) into Eq. (1), and integrating over volume we obtain

$$\frac{dN_{\mathrm{Rb}}}{dt} = L - \gamma N_{\mathrm{Rb}} - \frac{\beta_{\mathrm{Rb}} N_{\mathrm{Rb}}^2}{\omega_{\mathrm{Rb}}^3 \pi^{3/2}}. \tag{3}$$

This equation can be solved analytically. For MOT loading with initial condition $N(0) = 0$ one obtains [14]

$$N(t) = N_0\left[1 - \frac{(1+\xi)\exp(-t/\tau_L)}{1+\xi\exp(-t/\tau_L)}\right], \tag{4}$$

where

$$\tau_L = \frac{1-\xi}{1+\xi}\frac{1}{\gamma} \tag{5}$$

and

$$\xi = \left(1 + \sqrt{8}\frac{\gamma}{\beta n_0}\right)^{-1}. \tag{6}$$

The loading curves for each single-species MOT can be fit to Eq. (4) and the coefficients γ and β extracted with a least-squares fit.

With the values of γ and β determined, the interspecies trap loss rate coefficient β' can then be extracted. Substituting Eq. (2) into Eq. (1), this time keeping the β' term, and integrating over volume gives

$$\frac{dN_{\mathrm{Rb}}}{dt} = L - \gamma N_{\mathrm{Rb}} - \frac{\beta_{\mathrm{Rb}} N_{\mathrm{Rb}}^2}{\omega_{\mathrm{Rb}}^3 \pi^{3/2}} - \beta'_{\mathrm{Rb-Ar^*}} N_{\mathrm{Rb}} N_{\mathrm{Ar^*}} \left[\frac{2}{\pi(\omega_{\mathrm{Rb}}^2 + \omega_{\mathrm{Ar^*}}^2)}\right]^{3/2}. \tag{7}$$

The coefficient $\beta'_{\mathrm{Rb\text{-}Ar^*}}$ can be determined either by observing the difference in the transient loading of one MOT in the presence and absence of the second, loaded MOT, or by observing the steady-state behavior of the first MOT both with and without the second MOT present. For transient loading, the observed loading curve is fit to the solution of Eq. (7) to determine $\beta'_{\mathrm{Rb\text{-}Ar^*}}$.

The steady-state approach proceeds as follows: To determine $\beta'_{\mathrm{Rb\text{-}Ar^*}}$, we begin by recording the fluorescence loading curve of the Rb MOT without the presence of the Ar^* MOT (but with the Ar^* beam present). From this curve, we can extract N_{Rb}, γ, and β_{Rb} as described above. We further characterize the Rb MOT by using fluorescence or absorption imaging to measure the density profile and determine ω_{Rb}. Next, we allow the Ar^* MOT to load and record the number of Ar^* atoms, $N_{\mathrm{Ar^*}}$, and the Ar^* MOT size. Now with the Ar^* MOT present, we again measure the Rb MOT atom number N'_{Rb} and Rb MOT size. In steady state, $dN_{\mathrm{Rb}}/dt = 0$ and Eq. (7) leads to

$$\beta'_{\mathrm{Rb-Ar^*}} = \left[\frac{\pi(\omega'^2_{\mathrm{Rb}} + \omega^2_{\mathrm{Ar^*}})}{2}\right]^{3/2} \frac{1}{N'_{\mathrm{Rb}} N_{\mathrm{Ar^*}}} \times \left\{\gamma(N_{\mathrm{Rb}} - N'_{\mathrm{Rb}}) + \beta_{\mathrm{Rb}}\left[N_{\mathrm{Rb}}^2\left(\frac{1}{\pi\omega_{\mathrm{Rb}}^2}\right)^{3/2} - N'^2_{\mathrm{Rb}}\left(\frac{1}{\pi\omega'^2_{\mathrm{Rb}}}\right)^{3/2}\right]\right\}. \tag{8}$$

The identical procedure can be used to determine $\beta'_{\mathrm{Ar^*\text{-}Rb}}$. We have used the steady-state approach for determining the β' coefficients.

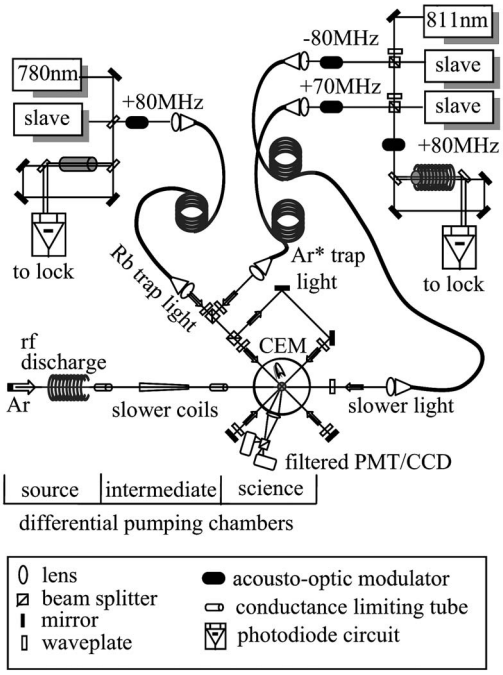

FIG. 1. Schematic of the apparatus.

III. EXPERIMENTAL APPARATUS

Our apparatus is similar to the one described in detail in Ref. [6]. Briefly, the dual MOT is produced in a stainless-steel, differentially pumped, vacuum chamber. Rubidium atoms are loaded into the MOT from a background vapor while metastable argon is loaded from an atomic beam. Metastable atoms are produced in a radio-frequency discharge which closely follows the design of Chen *et al.* [15] and passes through a Zeeman slower before entering the MOT region. Separate diode laser systems, operating in master-slave configuration, are used to cool and confine the Rb (780 nm) and Ar^* (811 nm). Both master lasers are locked to separate saturation absorption spectrometers. A schematic of the apparatus is shown in Fig. 1. The repumping frequency for the Rb MOT is obtained by direct modulation of the slave current through a bias T to produce sidebands at the required frequency [16]. Because ^{40}Ar does not have hyperfine structure, a repumper laser is not required for the Ar^* MOT.

IV. RESULTS AND DISCUSSION

When individually loaded, the Rb and Ar^* MOTs contain up to 2×10^6 and 1×10^6 atoms, respectively, in steady state. Both MOTs operate at a detuning of -2Γ, where Γ is the natural linewidth. A least-squares fit of the loading curve for Rb to the solution of Eq. (3) yields the following values: $\gamma_{\mathrm{Rb}} = (0.54\pm0.05)\ \mathrm{s}^{-1}$, $\beta_{\mathrm{Rb}} = (3.7\pm1.7)\times10^{-12}\ \mathrm{cm}^3/\mathrm{s}$, when the total intensity is $I = 20\ \mathrm{mW/cm}^2$. A fit to the corresponding equation for Ar^* yields $\gamma_{\mathrm{Ar^*}} = (0.73\pm0.26)\ \mathrm{s}^{-1}$, $\beta_{\mathrm{Ar^*}} = (5.8\pm1.7)\times10^{-10}\ \mathrm{cm}^3/\mathrm{s}$ when $I = 42\ \mathrm{mW/cm}^2$. The value of β_{Rb} is in line with previous measurements [17]. The high value of γ arises from the considerable background of

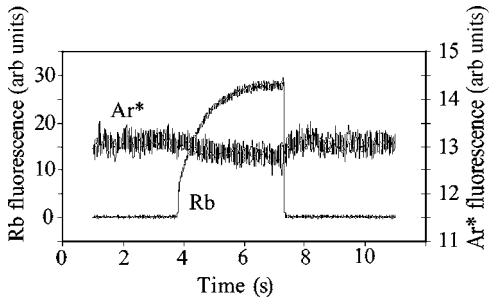

FIG. 2. Typical time evolution of Ar^* and Rb MOT fluorescence when the Rb MOT loads while spatially overlapped with an existing Ar^* MOT.

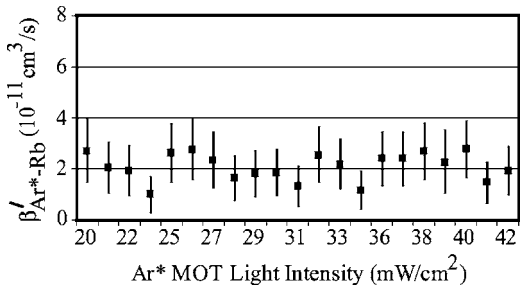

FIG. 3. 811-nm trap light intensity dependence of the interspecies trap loss coefficient $\beta'_{Ar^*\text{-}Rb}$, for the loss of Ar^* due to the presence of Rb.

ground-state Ar atoms that copropagate with the metastable argon beam.

In order to study interspecies trap loss, we must carefully overlap the Rb and Ar^* MOTs. Spatial overlap of both traps in three dimensions is assured by monitoring the fluorescence of each trap from two directions and with absorption imaging along one axis. Once overlap is confirmed, we allow the Rb MOT to load fully in the absence of the Ar^* MOT. Next, we allow the Ar^* MOT to load while we continue to monitor the Rb MOT fluorescence. When we do so, we find that there is a slight decrease of roughly 3% in the number of Rb atoms confined in the MOT. Similarly, we allow the Ar^* MOT to load fully in the absence of Rb, and then we allow the Rb MOT to load while we monitor the Ar^* MOT fluorescence. Again we find a modest decrease in the number of trapped atoms. A typical fluorescence curve is shown in Fig. 2. No difference in trap volume is observed for single or dual traps, consistent with our approximation that the trap loads at constant volume.

With the single-species and dual-species behavior characterized, we can use Eq. (8) to calculate the interspecies trap loss coefficient. With trap light intensities of 20 mW/cm^2 and 42 mW/cm^2 for ^{85}Rb and $^{40}Ar^*$, respectively, we find that the coefficient for the loss of Rb due to the presence of Ar^* is $\beta'_{Rb\text{-}Ar^*}=(3.0\pm1.3)\times10^{-11}$ cm^3/s and the reciprocal coefficient for the loss of Ar^* due to the presence of Rb is $\beta'_{Ar^*\text{-}Rb}=(1.9\pm0.9)\times10^{-11}$ cm^3/s.

In dual alkali-metal systems studied elsewhere, similar measurements have yielded a decrease of 20% in ^{39}K atoms when a ^{85}Rb MOT loads [18], a 45% decrease in ^{40}K when a ^{87}Rb MOT loads [19], and a 15% decrease in Na when a Rb MOT loads [20]. A review of recent heteronuclear trap loss measurements in dual alkali-metal systems can be found in Ref. [21]. Interestingly, in these experiments the reciprocal trap loss was usually found to be different. For example, no loss of Rb due to the presence of Na atoms was observed in Ref. [20] and no loss of ^{85}Rb due to the presence of ^{39}K atoms was observed in Ref. [18]. Here we have found the two loss rates to be comparable.

Light-assisted collisions can be a significant factor in trap loss, and trap loss rates are found, in general, to depend on intensity and detuning. Mechanisms for trap loss include fine- and hyperfine-state changing collisions and radiative escape. As the MOT light intensity increases, the recapture energy of the trap increases, but at the same time the excited-state fraction increases. It is an interplay between trap depth and excited-state trap loss which explains the intensity dependence of trap loss. These same mechanisms can contribute to heteronuclear trap loss. In addition, doubly-excited-state collisions of sodium atoms in a MOT can result in autoionization [22]. In metastable noble-gas traps, it is Penning and associative ionization which are mainly responsible for trap loss, and these processes can be enhanced or suppressed by near-resonant light [23,24]. Typical rate coefficients for Penning and associative ionization in metastable noble gas MOTs are $\beta\sim10^{-9}-10^{-10}$ cm^3/s. For helium, the rate can be greatly reduced by spin polarization of the atomic sample [25]; however, this suppression of ionization rates for heavier atoms disappears.

We have investigated, at fixed detuning, the dependence of the loss rate coefficients on trap light intensity. Operating at a detuning of -2Γ for both MOTs, we vary the intensity of the Ar^* 811-nm trap light over a range of 20–42 mW/cm^2 while holding the Rb 780-nm trap light constant at 20 mW/cm^2. The lower end of the intensity range was limited to stable trap operation. Results for $\beta'_{Ar^*\text{-}Rb}$ and $\beta'_{Rb\text{-}Ar^*}$ as a function of 811-nm trap light intensity are shown in Figs. 3 and 4, respectively. Error bars arise from the quality of the fit, the reproducibility of the data, and the estimated error in the determination of the number of trapped atoms and MOT volume. Similar data were taken for the reciprocal experiment where the Ar^* 811-nm light was held constant at 42 mW/cm^2 and the Rb 780-nm light was varied over a range of 15–20 mW/cm^2. Here we found that $\beta'_{Ar^*\text{-}Rb}\sim2\times10^{-11}$ cm^3/s, while $\beta'_{Rb\text{-}Ar^*}$ varied over a range of $2-3\times10^{-11}$ cm^3/s with little systematic variation over

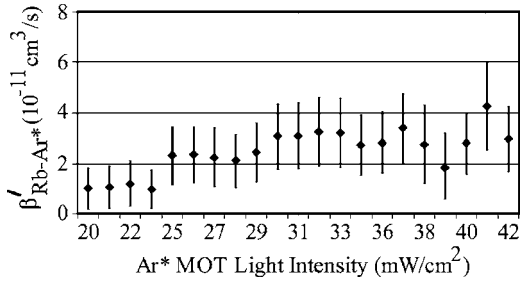

FIG. 4. 811-nm trap light intensity dependence of the interspecies trap loss coefficient $\beta'_{Rb\text{-}Ar^*}$, for the loss of Rb due to the presence of Ar^*.

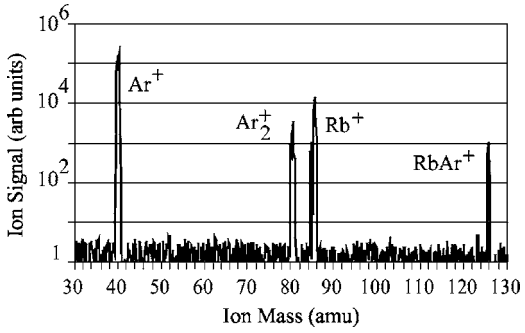

FIG. 5. Ion signal from the quadrupole mass spectrometer as a function of atomic mass.

the range of intensities studied and uncertainties comparable to those in Figs. 3 and 4.

Next we turn our attention to identifying the mechanism for the measured trap loss. Ultracold collisions between alkali-metal atom pairs in the ground ($nS+nS$) or first excited ($nS+nP$) molecular states do not have enough energy to result in ionization. For sodium, an atom pair in the second excited state ($3P+3P$) can autoionize and heteronuclear photoassociative ionization producing $NaCs^+$ has been observed [26]. A metastable noble-gas atom like Ar^*, however, contains more than enough internal energy to ionize a Rb atom. Ar^* lies 11.6 eV above the ground state, considerably more than the 4.2 eV ionization energy of rubidium. As a result, one would expect that heteronuclear ionization plays a role in alkali-metal–noble-gas trap loss.

In order to confirm that ionization plays a role in Rb-Ar^* MOT trap loss, we searched directly for ion products. One complication to ion detection is the large background of Ar^+ (Ar_2^+) ions produced in Penning (associative) ionization occurring in the Ar^* MOT alone. By comparison, for the trap loss observed here, ions produced in interspecies collisions are a negligible part of the total ion signal. To differentiate the ion products, we modified an SRS model 200 residual gas analyzer to act as a quadrupole mass spectrometer (QMS). Ion optics were placed in the MOT chamber to accelerate all ions produced in the MOT volume into the QMS where different mass products could be sorted. With only the Ar^* MOT present, Ar^+ and Ar_2^+ ions, arising from collision between ultracold Ar^* atoms in the MOT, are clearly identified by count peaks at 40 and 80 amu, respectively. With only the Rb MOT present, no ions are detected. When the Rb MOT is superimposed on the Ar^* MOT, additional peaks appear at 85 and 125 amu, corresponding to Rb^+ and $RbAr^+$, respectively, as shown in Fig. 5. This clearly identifies heteronuclear Penning and associative ionization as two of the mechanisms contributing to interspecies trap loss. Future absolute measurements of ion yield will enable us to specify the fraction of trap loss attributable to ionization. The details of the collision dynamics depend on the molecular energy-level structure. Although recent calculations of the long-range interaction between two metastable rare-gas atoms were reported [27], to the best of our knowledge, the structure of Rb+Ar^* has not been investigated theoretically.

In conclusion, we have measured the interspecies trap loss rate coefficients for ultracold collisions between Rb and Ar^* in a dual-species MOT and find the two rates to be approximately equal over the range of intensities studied. We have also measured the trap loss rate coefficient for cold collisions in a metastable argon MOT alone. Using a quadrupole mass spectrometer we observe the production of Ar^+, Ar_2^+, Rb^+, and $RbAr^+$ ions in the dual MOT, clearly identifying heteronuclear Penning and associative ionization as trap loss mechanisms. Future studies will focus on characterizing the molecular energy levels of Rb+Ar^* using photoassociative spectroscopy and on the production of ultracold, ground-state RbAr, a weakly bound van der Waals molecule.

ACKNOWLEDGMENTS

We gratefully acknowledge support from the National Science Foundation and the Office of Naval Research. We thank M.D. Havey for useful discussions.

[1] D. DeMille, Phys. Rev. Lett. **88**, 067901 (2002).
[2] M. Anderlini, E. Courtade, M. Cristiani, D. Cossart, D. Ciampini, C. Sias, O. Morsch, and E. Arimondo, Phys. Rev. A **71**, 061401(R) (2005).
[3] U. Schloder, C. Silber, and C. Zimmermann, Appl. Phys. B: Lasers Opt. **73**, 801 (2001).
[4] Z. Hadzibabic, C. A. Stan, K. Dieckmann, S. Gupta, M. W. Zwierlein, A. Gorlitz, and W. Ketterle, Phys. Rev. Lett. **88**, 160401 (2002).
[5] E. Bodo, F. A. Gianturco, and A. Dalgarno, J. Chem. Phys. **116**, 9222 (2002).
[6] C. I. Sukenik and H. C. Busch, Phys. Rev. A **66**, 051402(R) (2002).
[7] For a review of ultracold collisions, see J. Weiner, V. S. Bagnato, S. Zilio, and P. Julienne, Rev. Mod. Phys. **71**, 1 (1999).
[8] R. L. Cavasso-Filho, A. Scalabrin, D. Pereira, and F. C. Cruz, Phys. Rev. A **67**, 021402(R) (2003).
[9] G. D. Telles, W. Garcia, L. G. Marcassa, V. S. Bagnato, D. Ciampini, M. Fazzi, J. H. Muller, D. Wilkowski, and E. Arimondo, Phys. Rev. A **63**, 033406 (2001).
[10] C. D. Wallace, T. P. Dinneen, Kit-Yan N. Tan, T. T. Grove, and P. L. Gould, Phys. Rev. Lett. **69**, 897 (1992).
[11] D. Hoffmann, P. Feng, and T. Walker, J. Opt. Soc. Am. B **11**, 712 (1994).
[12] H. Katori and F. Shimizu, Phys. Rev. Lett. **70**, 3545 (1993).
[13] H. Kunugita, T. Ido, and F. Shimizu, Phys. Rev. Lett. **79**, 621 (1997).
[14] T. P. Dinneen, K. R. Vogel, E. Arimondo, J. L. Hall, and A. Gallagher, Phys. Rev. A **59**, 1216 (1999).
[15] C. Y. Chen, K. Bailey, Y. M. Li, T. P. O'Connor, Z.-T. Lu, X. Du, L. Young, and G. Winkler, Rev. Sci. Instrum. **72**, 271 (2001).
[16] R. Kowalski, S. Root, S. D. Gensemer, and P. L. Gould, Rev. Sci. Instrum. **72**, 2532 (2001).

[17] S. D. Gensemer, V. Sanchez-Villicana, K. Y. N. Tan, T. T. Grove, and P. L. Gould, Phys. Rev. A **56**, 4055 (1997).
[18] L. G. Marcassa, G. D. Telles, S. R. Muniz, and V. S. Bagnato, Phys. Rev. A **63**, 013413 (2000).
[19] J. Goldwin, S. B. Papp, B. DeMarco, and D. S. Jin, Phys. Rev. A **65**, 021402(R) (2002).
[20] Y. E. Young, R. Ejnisman, J. P. Shaffer, and N. P. Bigelow, Phys. Rev. A **62**, 055403 (2000).
[21] M. W. Mancini, A. R. L. Caires, G. D. Telles, V. S. Bagnato, and L. G. Marcassa, Eur. Phys. J. D **30**, 105 (2004).
[22] L. Marcassa, R. Horowicz, S. Zilio, V. Bagnato, and J. Weiner, Phys. Rev. A **52**, R913 (1995).
[23] K. A. Suominen, K. Burnett, P. S. Julienne, M. Walhout, U. Sterr, C. Orzel, M. Hoogerland, and S. L. Rolston, Phys. Rev. A **53**, 1678 (1996).
[24] H. Katori and F. Shimizu, Phys. Rev. Lett. **73**, 2555 (1994).
[25] N. Herschbach, P. J. J. Tol, W. Hogervorst, and W. Vassen, Phys. Rev. A **61**, 050702(R) (2000).
[26] J. P. Shaffer, W. Chalupczak, and N. P. Bigelow, Phys. Rev. Lett. **82**, 1124 (1999).
[27] A. Derevianko and A. Dalgarno, Phys. Rev. A **62**, 062501 (2000).